Tuijin Jishu/Journal of Propulsion Technology
ISSN: 1001-4055
Vol. 44 No. 5 (2023)

# Highly Accurate COVID Detection and Classification from CT and X-Ray Images Using Layer Recurrent Neural Network

**Ranjini Mupra P**
(Research Scholar, Department of Computer Application Annamalai University)

**Dr B Ashok**
Assistant Professor Division of Computer & Information ScienceAnnamalai University

**Dr Bindulal T S**
Assistant Professor Department of Computer ScienceGovernment College Nedumangaud Kerala

**Abstract**: - COVID-19 is a significant pandemic that severely attacked many countries. Studies state that earlier stage detection of COVID can reduce the risk of mortality to a great extent. Imposing artificial intelligence technology like Computer vision algorithms can be applied to observe chest X-rays and Computed Tomography (CT) images in order to predict the presence of coronavirus. CT and X-Ray images can provide clear information about the affected lungs and their fluid contents. In the present work, a Convolutional neural network-based technique is proposed to determine the COVID-19 prediction process. Initially, pre-processing is performed to increase the information level and reduce unwanted pixel noise by performing a suitable filtering process. In that stage, the contrast enhancement process equalizes the pixel values to increase the information level. A standard image database is used to perform training and testing processes separately. The system's performance is evaluated based on performancemetrics such as Accuracy, Sensitivity, and specificity.

**Keywords**: - COVID-19, Computer vision, Convolutional neural network, Deep Learning, contrast enhancement, sensitivity, and specificity.

## I. Introduction

Following the recent epidemic in China of a novel coronavirus (SARS-CoV-2, also known as 2019-nCoV), which was responsible for the coronavirus illness 2019 (COVID-19), the global public health community has been placed at considerable risk of infection. As of July 4, 2020, there were 11,191,872 laboratory-confirmed SARS-CoV-2-infected cases and 529,122 reported deaths all over the world, even though transportation to and from Wuhan and several other cities in China was shut down on January 23, 2020, to reduce virus transmission both in China and worldwide. The increasing seriousness of the problem could be attributed to a scarcity of appropriate Point-Of-Care Testing (POCT) assays for the prompt and accurate identification of SARS-CoV-2-infected patients in hospitals. Moreover, because asymptomatic and pre-asymptomatic SARS-CoV-2 infected patients are highly contagious, and because of a lack of appropriate detection assays, many SARS-CoV-2 infected patients have had contact with uninfected people before being identified and placed in home isolation or hospitalization[1].

The CT scan analysis revealed bilateral pulmonary parenchymal ground glass and consolidative pulmonary opacities, some of which had a rounded morphology and were distributed in the peripheral lung region of the patient. The COVID-19 diagnostic process, as a result, can be thought of as a challenge of image segmentation to extract the main characteristics of the disease. By constructing an algorithm that is capable of extracting smaller similar regions that can suggest infection with the COVID-19 virus, it is possible to overcome the segmentation challenge. Picture segmentation, or the separation of image portions from one another, is a critical step in image processing and computer vision because it allows image analysis techniques to focus on a specific region while boosting the accuracy of image analysis techniques

[2].

The COVID-19 test team is currently facing a severe issue due to the unavailability of the diagnosis system throughout the world, which is causing widespread worry. Because of the limited accessibility of COVID-19 testing units, forced to rely on a variety of other finding measures. Because COVID-19 affects the epithelial cells that line the walls of the respiratory system, use X-rays to assess the health of lung tissue. To diagnose any type of lungs ailment, the medical practitioner frequently uses X-ray pictures. It is also possible that, because practically all emergency clinics are equipped with X-ray machines, it may be possible to use an X-ray to detect COVID-19 without specialized test kits. As a result, developing anautomated analysis system is required to save medical personnel important time [3].

Even though immunological tests are also available in many countries, real-time reverse transcription-polymerase chain reaction (RT-PCR) is the most often used technique for COVID-19 identification. Images of the chest taken using radiological techniques such as CT scans and X-rays have played critical roles in this disease's prompt identification and early therapy. Because the RT-PCR has a low sensitivity of 60–70 percent and is also a time- consuming technology, diagnosing harmful effects of COVID-19 by reviewing images of the lungs of patients can ensure that patients receive therapy as soon as they are diagnosed. Remember that CT scanning is a more sensitive technique for diagnosing COVID-19 pneumonia and that it can be used in conjunction with RT-PRC to test for the virus in the first place. Pathological alterations in the lungs can be visible on a CT scan for a lengthy period after the onset of the symptoms [4].

Deep Learning techniques have seen a significant increase in popularity in recent years, and they have fundamentally transformed the landscape of several academic fields. Deep learning approaches, especially when applied to image data sets such as retinal images, chest X-rays, and brain MRIs, yield promising outcomes in the medical industry. To be a data scientist, one must be willing to train acquired photos with the importance of deep learning to provide significant aid to medical specialists in detecting COVID-19 patients. This is beneficial to develop countries that have access to X-ray facilities. Several deep learning classifiers have been demonstrated to be extremely effective in computer vision and medical image analysis applications, with Convolutional Neural Networks (CNN) being the most effective of these. The findings of CNN's mapping of picture data to a precise and predicted output have demonstrated the accuracy with which it performs this mapping. Because the lungs are the primary site of infection for the virus, examining their alterations can provide a definitive indication of the virus' existence [5].

The major analysis contributions of this paper are summarized as follows:

- Proposed an algorithm to detect the COVID-19 patients using X-ray and CT images.
- To improve the classification accuracy of COVID-19 patients from X-ray and CT images

The structure of this work is orderly as, in section II, the details of the previous work are explained. In section III, the proposed techniques with feature extraction, optimization, and classification are explained detailed manner. In section IV, shows the result and discussions with various performance matrices. At last, section V concludes this work.

## II. Literature Survey

From the perspective of feature extraction and combination, several relevant COVID detection studies have been published earlier. In brief, the existing related works reviews are as follows: El-Sayed M. El-Kenawy et al. [6] proposed a classification method with two stages to classify different cases from chest X-ray images based on a proposed Advanced Squirrel Search Optimization Algorithm; El-Sayed M. El-Kenawy et al. proposed a classification method with two stages to classify different cases from chest X-ray images based on (ASSOA). The feature learning and extraction operations are carried out in the first stage using a CNN model termed ResNet-50, which is combined with image augmentation and dropout processes. After that, the ASSOA method is used to the recovered features to facilitate the feature selection process. Finally, the suggested ASSOA algorithm (using the specified characteristics) is used to optimize the connection weights of the Multi-layer Perceptron (MLP) Neural Network, which is then used to classify the input cases. The studies make use of a Kaggle chest X-ray pictures (Pneumonia) dataset, which contains 5,863 X-rays and was created by Kaggle. The proposed (ASSOA C MLP) method attained a classification mean accuracy of 99.26

percent, which is an impressive result.
Julián D. Arias-Londoo et al. built the COVID-Net network, which was used to develop an architecture that was more polished in the following years. This network was chosen because of its specialized properties and because of the positive outcomes produced by other researchers in the past with this network. To train the COVID-Net, it was necessary to use a corpus of data obtained from several sources, including data from the control and pneumonia classes [7], which had 49, 983 and 241, 114 samples, respectively.

Mehmet Yamaç and colleagues presented a method to distinguish between three types of COVID-19 patients: those with bacterial pneumonia, those with viral pneumonia, and those with normal lung function. To conduct this research, a benchmark COVID-19 X-ray data set, Qata-Cov19 (Qatar University and Tampere University COVID-19 Data set), was assembled, which contains 462 X-ray pictures from COVID-19 patients. The photos in the data set differ in terms of quality, resolution, and signal-to-noise ratio (SNR). When using them for COVID- 19 detection, data scarcity can be a significant stumbling block. Even though representation- based classification [collaborative or Sparse Representation (SR)] may provide excellent performance with small data sets, it is generally agreed that these approaches fall short in terms of performance and speed when compared to the Neural Network (NN)-based methods. A Convolution Support Estimation Network (CSEN) has been proposed as a bridge between representation-based and neural network approaches [8]. It does so by providing a noniterative real-time mapping from query sample to ideally SR coefficient support, which is critical information for class decisions in representation-based techniques.

In this paper, Changjian Zhou et al. investigated the COVID-19 chest X-ray images and developed a combined method of image regrouping and ResNet-SVM to analyze the images. This image was created by segmenting and dividing the lung region from the original chest X- ray images, and then randomly reassembling the split and reassembling the lung region to create an image that looked like the original image. The regrouped photos were also put into the deep residual encoder block, which was used to extract features from the images. Finally, the collected features were sent into a support vector machine for recognition, which produced a positive result. The unique strategy included the introduction of visual attention, which focused greater attention on the characteristics of COVID-19 while eliminating distraction from forms, ribs, and other related noises. Using only a small number of training data, the proposed technique attained 93 percent accuracy, according to the experimental results [9].

To distinguish COVID-19 infection from normal and other pneumonia cases using chest X-ray pictures, Chaimae Ouchicha et al. developed a unique deep learning architecture based on CNN architecture, called CVDNet. The first step is to formalize the operations that are performed by the network. The model was trained on a tiny dataset consisting of a few photos of diverse COVID-19, viral pneumonia, and normal cases obtained from a publicly accessible source. Furthermore, the classification efficiency of CVDNet was assessed by the use of k-fold cross- validation techniques. According to the findings, CVDNet achieved an average accuracy of 97.20 percent for detecting COVID-19 and an average accuracy of 96.69 percent for three- class classification (COVID-19, normal pneumonia, and viral pneumonia), demonstrating superior and promising performance in categorizing COVID-19 cases. As a result of these encouraging findings, a CVDNet model is an intriguing tool that can assist doctors in diagnosing and detecting COVID-19 infection in a relatively short period. In the future, researchers attempt to construct CVDNet, which allows them to distinguish COVID-19 cases from those caused by other lung disorders. Want to verify the proposed model using additional images received from various hospitals, as well as to address CT images for the identification of COVID-19 and compare the findings with the CVDNet trained on X-ray images [10]. However, the above-mentioned methods have merits and demerits. The main disadvantage of the previous works is computation time and accuracy. The main purpose of this work is toovercome the shortcomings of the previous work.

1. To reduce the complexity of the detection process that increases the capability of thereal-time testing process.
2. To improve the accuracy of the detection process by maintaining the image pre-processing and feature extraction techniques.

The details of the implementation of the projected work area unit are given below sections.

---

### III. COVID Detection and Classification from CT and X-Ray Images UsingDeep CNN

The x-ray and CT scan images are taken from the database and then the images are resized into224x224. After the resizing, the images are denoised and normalized. after the pre-processing,the image can be segmented by the affected area. Then feature extraction methods are a statistical feature, CSLBP, and edge feature are applied. Finally, the cascade feature is trainedand tested. Fig.1. shows the block diagram of COVID detection and classification from CT andX-Ray Images using LRNN

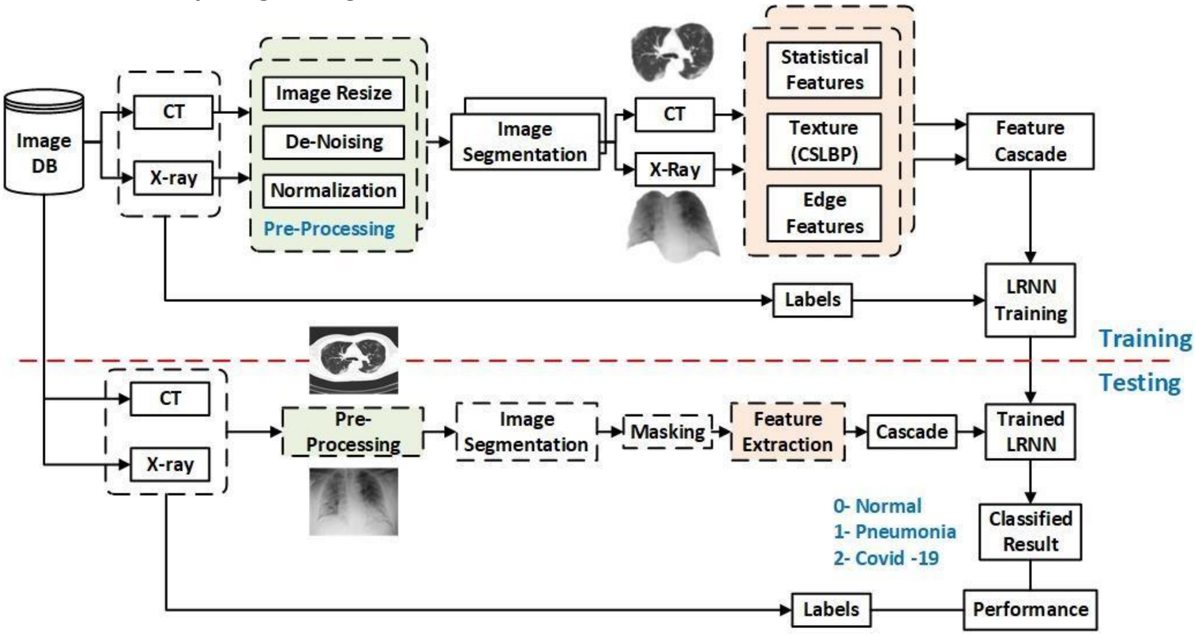


**Fig.1.Block diagram of COVID Detection and Classification from CT and X-Ray Images Using LRNN**

### A. Data pre-processing

Because the data set is not uniform and the By-ray images are of varying sizes, transformed all of the photos to the same size of 224 x 224 pixels to make them all look the same. To do this, RGB reordering has been applied, and the final input to the suggested model is presented as a picture with the dimensions 224x224x3. It has been noted that the data set is limited, and as a result, denoising and normalization have been conducted on the data. Now, this data collection may be used to train on more images with the same data set than it could previously.

### B. Feature Extraction

#### 1. Statistical Features

Standard Deviation: In statistics, the standard deviation is a measure of the variance of the distribution of a set of values. A low standard deviation means that values are usually set as means, while higher standard deviations are spread over a wide range. The formula for the sample standard deviation is

$$s = \sqrt{\frac{1}{N-1}\sum_{i=1}^{N}(x_i - \bar{x})^2} \quad (1)$$

where $\{x_1, x_2 \ldots x_n\}$ are the observed values of the sample items, $\bar{x}$is the mean value of these observations, N is the number of observations of the sample.

Mean: Mean is a set of observed data is defined as being equal to the sum of the numericalvalues of every observation, divided by the total number of observations. The arithmetic means of a set of numbers $x_1, x_2, ..., x_n$ is typically denoted by $\bar{x}$sample n is the number of items in the

$$\bar{x} = \frac{1}{n}\left(\sum_{i=1}^{n} x_i\right) = \frac{x_1 + x_2 + \cdots + x_n}{n} \tag{2}$$

Kurtosis: In probability theory and statistics, kurtosis is a measure of the "tailedness" of the probability distribution of a real-valued random variable. Like skewness, kurtosis describes the shape of a probability distribution and related methods for estimating it based on a sampleof the population. The kurtosis is the fourth standardized moment, defined as

$$\mathrm{Kurtosis}[X] = E\left[\left(\frac{X-\mu}{\sigma}\right)^4\right] = \frac{E[(X-\mu)^4]}{(E[(X-\mu)^2])^2} = \frac{\mu_4}{\sigma^4} \tag{3}$$

where μ4 is the fourth central moment and σ is the standard deviation. K denotes the kurtosis. Skewness: In probability theory and statistics, skewness is a measure of the asymmetry of the probability distribution of a real-valued random variable relative to its mean. The skewness value can be positive, zero, negative, or undefined.

The skewness of a random variable X is the third standardized moment $\tilde{\mu}_3$ defined as:

$$\tilde{\mu}_3 = E\left[\left(\frac{X-\mu}{\sigma}\right)^3\right] = \frac{\mu_3}{\sigma^3} = \frac{E[(X-\mu)^3]}{(E[(X-\mu)^2])^{3/2}} = \frac{\kappa_3}{\kappa_2^{3/2}} \tag{4}$$

where μ is the mean, σ is the standard deviation, E is the expectation operator, μ3 is the third central moment, and κt is the t-th cumulants. The last equality expresses skewness in terms of the ratio of the third cumulant κ3 to the 1.5th power of the second cumulant κ2.

Moment: The Moment concept is used in mechanics and statistics. If the function represents mass, then the zeroth moment is the total mass, the first moment divided by the total mass is the center of mass, and the second moment is the rotational inertia. If the function is a probability distribution, then the zeroth moment is the total probability (i.e. one), the first moment is the expected value, the second central moment is the variance, the third standardized moment is the skewness, and the fourth standardized moment is the kurtosis.

The n-th moment of a real-valued continuous function f(x) of a real variable about a value c is

$$\mu_n = \int_{-\infty}^{\infty} (x-c)^n f(x)\, dx \tag{5}$$

## 2. CSLBP (C-SYMMETRIC LOCAL BINARY PATTERNS)

It computes the histogram of the CSLBP operator, which is an extension of the LBP operator. Using CSLBP is useful for transforming photos that are both light and drab in appearance. Thus, the CSLBP histogram is extraordinarily long because of this factor. Please keep in mind that it is used as a description for a critical point in the document. Calculate a local patch around the key points, and then compute the CSLBP descriptor based on the key points and the local patch. However, for the sake of simplicity. It is only the comparison style between pixels that are altered by CSLBP. CSLBP compares center-symmetric pairs of pixels, rather than comparing surrounding pixels with the center pixel, as opposed to other approaches. Fig. 2 shows the structure of CSLBP. The CSLBP descriptor can be computed as follow

$$CSLBP_{r,p} = \sum_{i=0}^{\frac{p}{2}-1} f\left(\left|g_i - g_{i+\frac{p}{2}}\right|\right) 2^i, \quad f(x) = \begin{cases} 1 & \text{if } x \geq \tau \\ 0 & \text{otherwise} \end{cases} \tag{6}$$

Tuijin Jishu/Journal of Propulsion Technology
ISSN: 1001-4055
Vol. 44 No. 5 (2023)

where r is the radius of the circle, p is the number of sampled points in the circle, W is a small threshold used to limit the difference between center-symmetric pairs of pixels, $g_i$ and $g_{i+p/2}$ are the gray-scale value of center-symmetric pairs of pixels

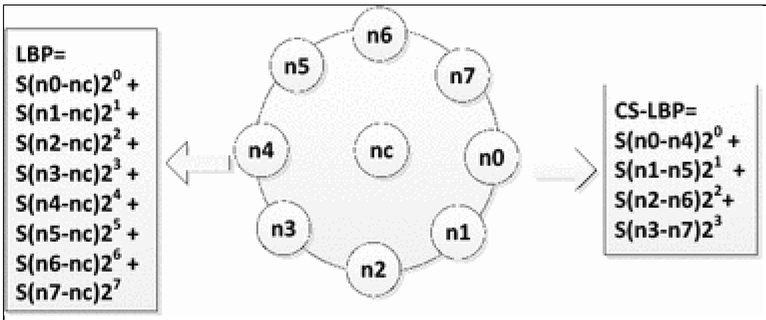


**Fig. 2. The structure of CSLBP**

## C. Layer Recurrent Neural Network

In the Layer-Recurrent Neural Network, there is a feedback loop, with a single delay, around except for the last layer of the network, each layer of the network A transfer function is utilized for the hidden layer and an output layer in the original Elman network, which had only two layers in the beginning. A form of Layer Recurrent Neural Network capable of learning order dependence in sequence prediction tasks, Long Short-Term Memory (LSTM) networks is a type of Layer Recurrent Neural Networks. Such behavior is essential in complicated problem areas such as machine translation, speech recognition, and other similar applications. Deep learning is a complicated field, and LSTM is one of the most sophisticated. It can be difficult to grasp the concept of LSTMs, as well as how words such as bidirectional and sequence-to- sequence apply to the subject of machine learning. Nobody, including the specialists who designed LSTMs, is better at clearly and accurately expressing both the promise of LSTMs and the way they work than those who produced them.

The Layer Recurrent Neural Network contains two test methods to check:

- ➢ number of LSTM parameters,
- ➢ output and cell states of the LSTM cell for two iterations.

The first method implements the validation of the correct number of LSTM parameters. The LSTM cell has three types of matrices: U, W, and B for each LSTM component: forget gate, input gate, output gate, and cell update. Let us assume the number of input dimensions is n, and the number of output dimensions is m. Also, let assume that the dimension number of thecell is equal to the output dimension. To define the following matrices:

- o U matrix with dimensions of m x n
- o W matrix with dimensions of m x m
- o B matrix (vector) with dimensions 1xmIn total the LSTM has

$$P_{(LSTM)} = 4(m^2 + mn + m) \quad (7)$$

Where $P_{(LSTM)}$ is the number of parametersThe LSTM has the following Layers

**Sequence Input Layer:** A sequence input layer inputs sequence information to a network.LSTM Layer: outlined by hidden state dims and a variety of layers

Fully Connected Layer: That maps the output of the LSTM layer to the desired output size. Softmax Layer: A softmax layer, allows the neural network to run a multi-class function. Inshort, the neural network is now able to determine the probability that the dog is in the image,as well as the probability that additional objects are included as well.

Classification Layer: A classification layer computes the cross-entropy loss for multi-class classification issues with reciprocally exclusive categories. The layer infers the number of categories from the output size of the previous layer.

The detailed structure is shown in Fig. 3 for the basic LSTM unit. Three gate controllers are placed into the LSTM unit, namely the input, forget and output gates. The three gates are mainly used to determine what information should be remembered. The LSTM network implements temporal memory through the switch of the gates to prevent the gradient from vanishing For the basic LSTM unit, its external inputs are its previous cell state $c_{(t-1)}$, the previous hidden state $h_{(t-1)}$th and the current input vector $x_{(t)}$.

The LSTM has the following Layers

$$f_{(t)} = \sigma(w_{fx}x_{(t)} + w_{fh}h_{(t-1)} + b_f) \tag{8}$$

$$i_{(t)} = \sigma(w_{ix}x_{(t)} + w_{ih}h_{(t)} + b_i) \tag{9}$$

$$o_{(t)} = \sigma(w_{ox}x_{(t)} + w_{oh}h_{(t-1)} + b_o) \tag{10}$$

where σ is the nonlinear activation function. Usually, the sigmoid function can be used as an activation function for the gates. Inside the LSTM, an intermediate state $c_{(t)}$is generated as

$$c_{(t)} = tanh(w_{cx}x_{(t)} + w_{ch}h_{(t-1)} + b_c) \tag{11}$$

Where $w_{fx}, w_{ix}, w_{ox}, w_{cx}$ are the input weights, $w_{fh}, w_{ih}, w_{oh}, w_{ch}$, are the recurrent

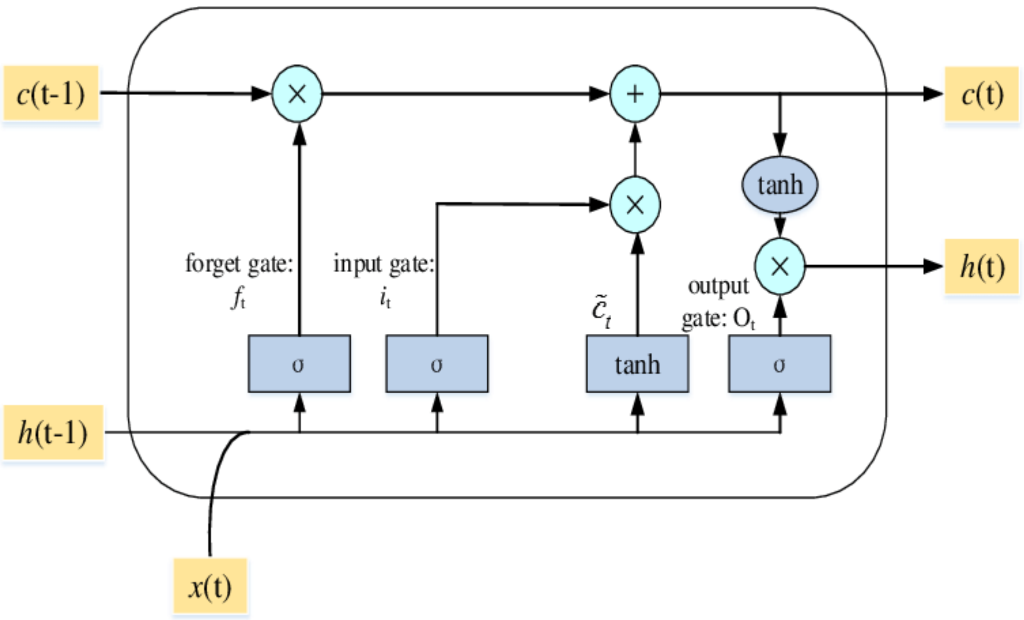


weights, and the $b_f, b_i, b_o, b_c$ are the biases.

**Fig.3. Structure of LSTM**

## IV. Results and Discussions

In this study, the performance of classification models for the identification of COVID19 was evaluated using an eleven-model CNN ensemble. The experimental studies were carried out with the help of the MATLAB 2019a deep learning toolbox, which can be downloaded here. Everything was done using a laptop, namely, an Acer Predator Helios 300 Core i5 8th Gen - (8 GB/1 TB HDD/128 GB SSD/Windows 10 Home/4 GB Graphics), which was outfitted with an NVIDIA GeForce GTX 1050Ti graphics card. The accuracy, sensitivity, specificity, false- positive rate (FPR), F1 Score, MCC, and Kappa of each classifier are all quantified in terms ofaccuracy, sensitivity, and specificity.

### A. Data set collection

Computational methods such as AI, Data Science, Machine Learning, and data mining are being used actively to obtain an effective solution to the COVID-19 pandemic. These ways square measure in the main captivated with the datasets for creating a good detection. Since COVID-19 is a new disease therefore a limited number of datasets is available for the executionof experiments. However, to apply deep learning to radiology imaging, few public datasets areavailable.

- SARS-COV-2 CT-scan dataset is collected from a hospital in Sao Paulo, Brazil, and approved by their ethical committee. It consists of 1252 CT-Scans of COVID-19 positive patients and 1230 CT-Scans for NON-COVID patients who are COVID-19 negative but may have other pulmonary diseases.

- Chest X-ray Images (Pneumonia) dataset has a large number of publicly available OCT and CXR images. In the experiments, used the X-Rays part of this dataset which consists of 5856 images of Pneumonia and Normal patients.
- COVID-chest X-ray-dataset dataset and is being used widely by many researchers. It consists of 673 radiology images of 342 unique patients. These radiology images include various CXR and CT scans of COVID-19 infected patients and with other pulmonary diseases too. After selecting the unique cases of COVID-19 positive patients the total number of patients reduces to 285 along with a total number of images to 526. The CXR offered during this dataset will be categorised into three different categories known as Posteroanterior (PA), Anteroposterior (AP), and AP Supine (APS).

The use of this dataset ensures the issue of data leakage as there are different unique patients, having more than one sample of CXR or CT-Scan images available in the datasets. Therefore, while splitting the dataset for training and testing purposes, and addressing the issue of data leakage, then a single patient CXRs or CT-Scans could end up in both testing and training giving false results.Fig.4. shows some examples of X-ray images of normal, pneumonia, and COVID and Fig.5. shows the CT images of non-COVID and COVID images.

| | | |
|---|---|---|
|  | 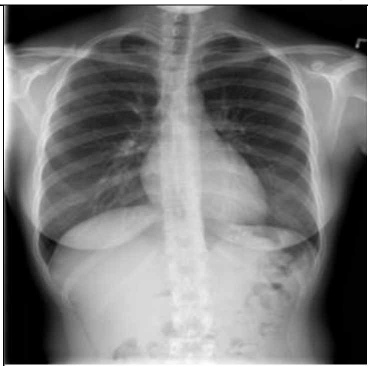 |  |
| (a) | (b) | (c) |
|  |  | 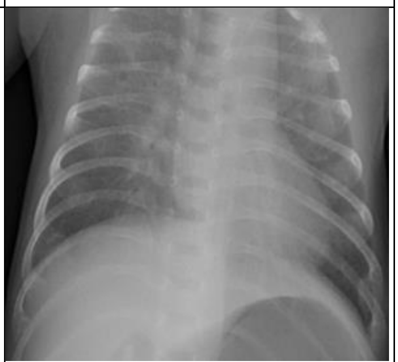 |
| (d) | (e) | (f) |

(g) (h) (i)

**Fig.4. (a), (b), (c) normal X-ray images (d), (e), (f) pneumonia X-ray images (g), (h), (i) COVID X-ray images**

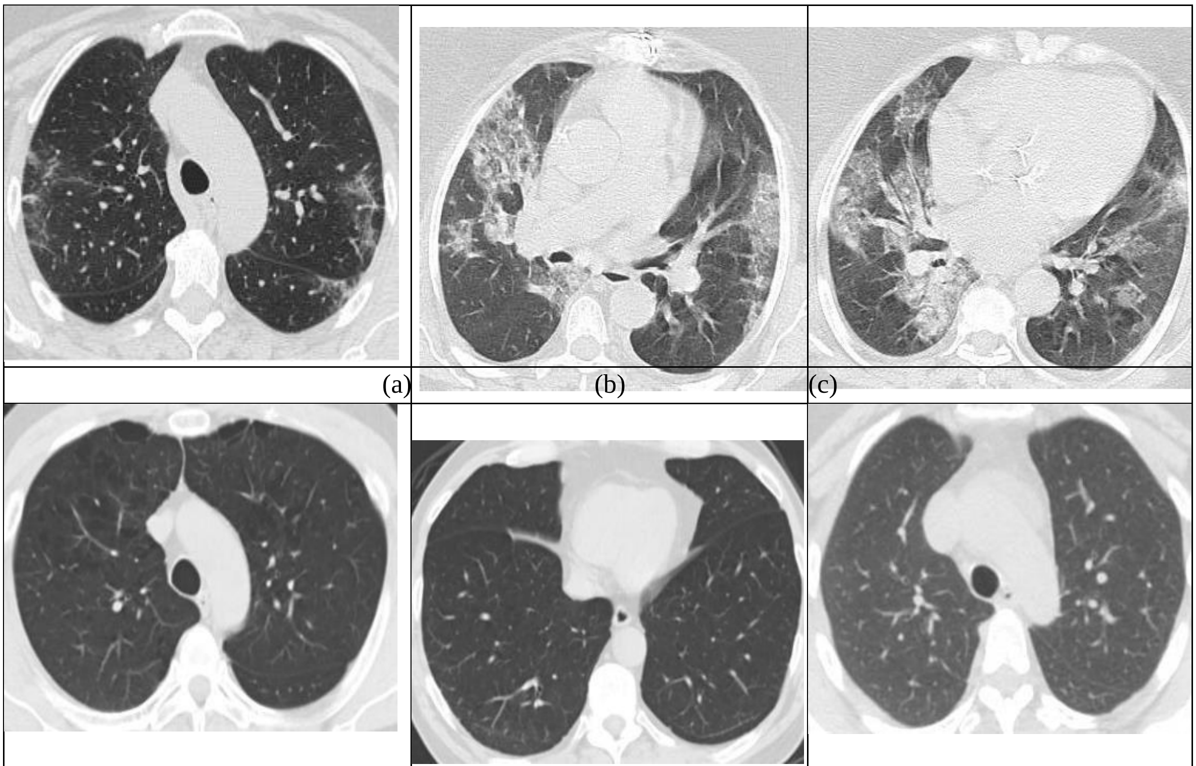

**Fig.5. (a), (b), (c) COVID CT scan images (d), (e), (f) non- COVID CT scan images**

**B. Classification Performance**

Classification performance is the metric used to evaluate the quality of the framework. Here the performance is measured in terms of accuracy, sensitivity, specificity, precision, and recall.**Accuracy**

Accuracy is used as the evaluation metrics for the multi-class classification. The accuracy is defined by the following equation.

$$ACC(i) = \sum^{N} \frac{Acc(m)}{N_m} \quad (12)$$

$m=1$

Where $ACC(i)$ is the accuracy of the i[th]class, and $N_m$is the number of samples in the m[th] class

**False Positive (FP)**

It is an extent of negatives samples that are inaccurately delegated as positive. Let us consider $\alpha(m)$ as the misclassified sample from the m[th] class. $\delta_m$is the false sample from m[th] class then the false positive is given by the following equation.

$$FP = \frac{1}{K}\sum_{m=1}^{K} \frac{\alpha(m)}{\delta_m} \quad (13)$$

**Sensitivity**

The sensitivity of a test relates to its capacity to appropriately identify patients who have thecondition. Mathematically, it can be expressed as:

$$Sensitivity = \frac{Number\ of\ true\ positives}{Number\ of\ true\ positives + Number\ of\ false\ negatives} \quad (14)$$

**Specificity**

The specificity is the ability of a test to correctly identify those patients without the disease.

$$\text{Specificity} = \frac{\text{Number of true negatives}}{\text{Number of true negatives+Number of false positives}} \quad (15)$$

**Precision**

The ratio of positive and negative outcomes in statistical and diagnostic tests to positive and negative results are the positive and negative precision values, respectively. The precision is defined as:

$$\text{Precision} = \frac{\text{Number of TP}}{\text{Number of TP+Number of FP}} = \frac{\text{Number of TP}}{\text{Number of positive calls}} \quad (16)$$

Where TP=True Positive; FP=False Positive

Table.1. depicts the training Parameters of the COVID detection and classification from CT and X-Ray Images using LRNN Table.2. shows the performance of proposed method based on the datasets. Table.3. shows the comparison of proposed method with previous methods.

**Table.1. Training Parameters of the proposed method**

| | |
|---|---|
| Number of training images | 200 |
| Number of testing images | 100 |
| Number of epochs | 100 |
| Iterations | 10 |
| Number of hidden units | 100 |
| Number of classes | 03 |
| Minimum Batch size | 50 |

**Table.2. Performance of proposed method**

| Performance | X-ray | CT | X-ray+CT |
|---|---|---|---|
| Accuracy | 97.69 | 98.63 | 99.82 |
| Sensitivity | 94.25 | 98.46 | 98.2 |

| | | | |
|---|---|---|---|
| Specificity | 97.81 | 97.51 | 99.53 |
| Precision | 89.42 | 93.28 | 92.38 |

**Table.3. Comparison with previous methods**

| Method | Accuracy | Sensitivity | Specificity | Precision |
|---|---|---|---|---|
| [11] | 87.02 | 85.35 | 92.18 | 89.96 |
| [12] | 99.4 | 99.3 | 99.2 | |
| [13] | 98.97 | 89.39 | 99.75 | |
| [14] | 89.50 | 87.00 | 88.00 | |
| [15] | 92.64 | 91.37 | 95.76 | |
| This method | 99.82 | 98.2 | 99.53 | 92.38 |

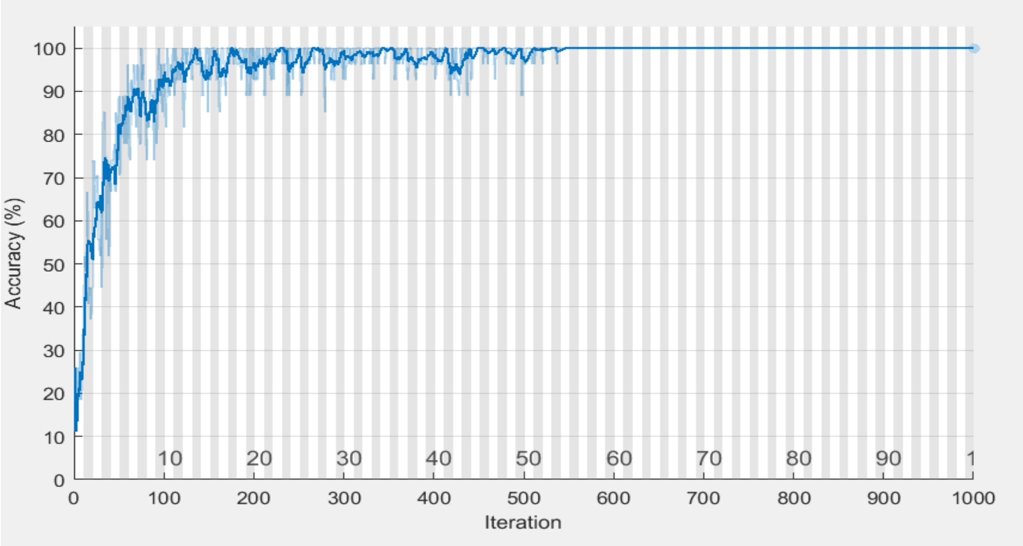


**Fig.6.Training and validation accuracy graph of the proposed method**

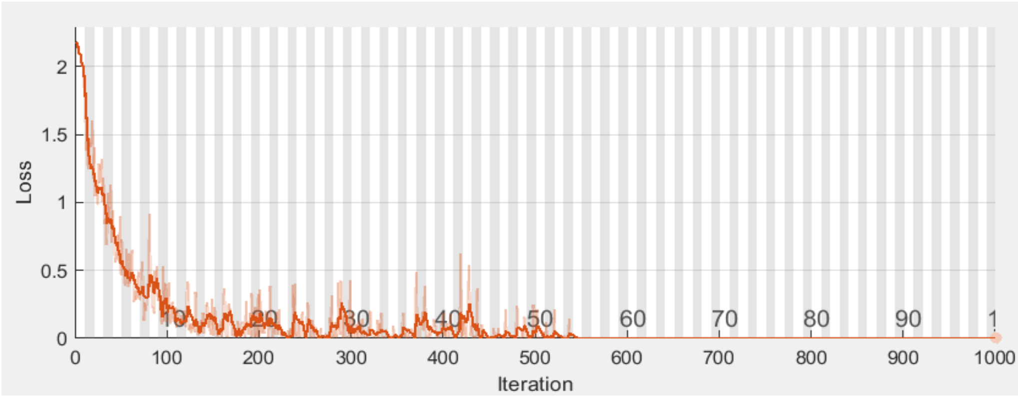


**Fig.7. Training and validation loss value graph of the proposed method**

Fig.6. shows the training and validation accuracy graph of the proposed method Fig.7. displays the training and validation loss value graph of the proposed method. Fig.8. depicts confusion chart for the proposed method.

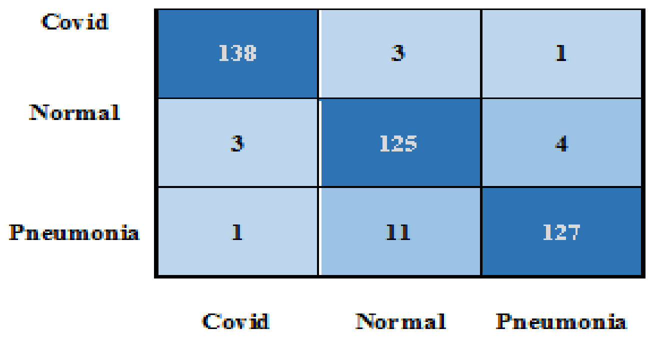


**Fig.8. Confusion chart for the proposed method**

## IV. Conclusion

The most generally used approaches in COVID-19 diagnosis, particularly RT-PCR and CT, have some limitations and downsides, such as long processing times and unacceptably high rates of misdiagnosis, which must be addressed. Due to a shortage of data from the COVID-19 examples, these disadvantages are shared by the majority of recent efforts in the literature that use deep learning to solve problems. However, even though deep learning-based recognition algorithms are prominent in computer vision where they have attained state-of-the-art performance, their performance declines rapidly owing to data scarcity, which is the reality of the problem under consideration. The goal of this study is to overcome these constraints by providing a robust and highly accurate COVID-19 recognition approach that can be used directly to X-ray image data. The suggested methodology is based on the CSEN, which can be thought of as a transitional state between deep learning models and representation-based approaches. CSEN learns a direct mapping from the query samples to the sparse support set of representation coefficients by using both a dictionary and a set of training samples in conjunction with each other. With this one-of-a-kind capability and the advantage of a compact network, the suggested CSEN-based COVID-19 identification systems outperform competing methods, achieving greater than 98 percent sensitivity and greater than 95 percent specificity in comparison to them. Furthermore, they produce the scheme that is the most computationallyefficient in terms of speed and memory.

## Reference

[1] Ji, Tianxing, Zhenwei Liu, GuoQiang Wang, Xuguang Guo, Changchun Lai, Haoyu Chen, Shiwen Huang et al. "Detection of COVID-19: A review of the current literature and future perspectives." Biosensors and Bioelectronics 166 (2020): 112455.

[2] Abdel-Basset, Mohamed, Reda Mohamed, Mohamed Elhoseny, Ripon K. Chakrabortty, and Michael Ryan. "A hybrid COVID-19 detection model using an improved marine predator’ algorithm and a ranking-based diversity reduction strategy."IEEE Access 8 (2020): 79521-79540.

[3] Sethy, Prabira Kumar, and Santi Kumari Behera. "Detection of coronavirus disease (COVID-19) based on deep features." (2020).

[4] Hussain, Emtiaz, Mahmudul Hasan, Md Anisur Rahman, Ickjai Lee, Tasmi Tamanna, and Mohammad Zavid Parvez. "CoroDet: A deep learning based classification for COVID-19 detection using chest X-ray images." Chaos, Solitons & Fractals 142 (2021): 110495.

[5] Panwar, Harsh, P. K. Gupta, Mohammad Khubeb Siddiqui, Ruben Morales-Menendez, and Vaishnavi Singh. "Application of deep learning for fast detection of COVID-19 in X-Rays using nCOVnet." Chaos, Solitons & Fractals 138 (2020): 109944.

[6] El-Kenawy, El-Sayed M., Seyedali Mirjalili, Abdelhameed Ibrahim, Mohammed Alrahmawy, M. El-Said, Rokaia M. Zaki, and Marwa Metwally Eid. "Advanced Meta- Heuristics, Convolutional Neural Networks, and Feature Selectors for Efficient COVID-19 X-Ray Chest Image Classification." IEEE Access 9 (2021): 36019-36037.

[7] Arias-Londoño, Julián D., Jorge A. Gomez-Garcia, Laureano Moro-Velázquez, and Juan I. Godino-Llorente. "Artificial Intelligence applied to chest X-Ray images for the automatic detection of COVID-19. A thoughtful evaluation approach." IEEE Access 8(2020): 226811-226827.

[8] Yamaç, Mehmet, Mete Ahishali, Aysen Degerli, Serkan Kiranyaz, Muhammad EH Chowdhury, and Moncef Gabbouj. "Convolutional Sparse Support Estimator-Based COVID-19 Recognition From X-Ray Images." IEEE Transactions on Neural Networksand Learning Systems 32, no. 5 (2021): 1810-1820.

[9] Zhou, Changjian, Jia Song, Sihan Zhou, Zhiyao Zhang, and Jinge Xing. "COVID-19 Detection based on Image Regrouping and ResNet-SVM using Chest X-ray Images." IEEE Access (2021).

[10] Ouchicha, Chaimae, Ouafae Ammor, and Mohammed Meknassi. "CVDNet: A novel deep learning architecture for detection of coronavirus (COVID-19) from chest x-ray images." Chaos, Solitons & Fractals 140 (2020): 110245.

[11] Ozturk, Tulin, Muhammed Talo, Eylul Azra Yildirim, Ulas Baran Baloglu, Ozal Yildirim, and U. Rajendra Acharya. "Automated detection of COVID-19 cases using deep neural networks with X-ray images." Computers in biology and medicine 121 (2020): 103792.

[12] Islam, Md Zabirul, Md Milon Islam, and Amanullah Asraf. "A combined deep CNN- LSTM network for the detection of novel coronavirus (COVID-19) using X-ray images." Informatics in medicine unlocked 20 (2020): 100412.

[13] Nour M., Cömert Z., Polat K. A novel medical diagnosis model for COVID-19 infection detection based on deep features and Bayesian optimization. Appl. Soft Comput. J. 2020;97 doi: 10.1016/j.asoc.2020.106580

[14] Wang S., Kang B., Ma J., Zeng X., Xiao M., Guo J., Cai M., Yang J., Li Y., Meng X., Xu B. 2020. A deep learning algorithm using CT images to screen for corona virus disease (COVID-19) MedRxiv.

[15] Wang L., Lin Z.Q., Wong A. COVID-Net: a tailored deep convolutional neural network design for detection of COVID-19 cases from chest X-ray images. Sci. Rep. 2020;10 doi: 10.1038/s41598-020-76550-z.